Tribology Letters (2023) 71:12
https://doi.org/10.1007/s11249-022-01686-0

ORIGINAL PAPER

The Flow of Lubricant as a Mist in the Piston Assembly and Crankcase of a Fired Gasoline Engine

Christopher J. Dyson[1] · **Martin Priest**[2] · **Peter M. Lee**[3]

Received: 20 October 2022 / Accepted: 2 December 2022 / Published online: 9 December 2022

Abstract
The tribological performance of the piston assembly of an automotive engine is highly influenced by the complex flow mechanisms that supply lubricant to the upper piston rings. As well as affecting friction and wear, the oil consumption and emissions of the engine are strongly influenced by these mechanisms. There is a significant body of work that seeks to model these flows effectively. However, these models are not able to fully describe the flow of lubricant through the piston assembly. Some experimental studies indicate that droplets of lubricant carried in the gas flows through the piston assembly may account for some of this. This work describes an investigation into the nature of lubricant misting in a fired gasoline engine. Previous work in a laboratory simulator showed that the tendency of a lubricant to form mist is dependent on the viscosity of the lubricant and the type and concentration of viscosity modifier. The higher surface area-to-volume ratio of the lubricant if more droplets are formed or if the droplets are smaller is hypothesised to increase the degradation rate of the lubricant. The key work in the investigation was to measure the size distribution of the droplets in the crankcase of a fired gasoline engine. Droplets were extracted from the crankcase and passed through a laser diffraction particle sizer. Three characteristic droplet size ranges were observed: Spray sized (250–1000 µm); Major mist (30–250 µm); and Minor mist (0.1–30 µm). Higher base oil viscosity tended to reduce the proportion of mist-sized droplets. The viscoelasticity contributed by a polymeric viscosity modifier reduced the proportion of mist droplets, especially at high load.

Keywords Crankcase lubricant · Droplet formation · Viscosity modifiers · Viscosity index improvers · Droplet size distribution · Laser diffraction particle size measurement

1 Introduction

For many years, researchers addressing various aspects of automotive engines have been aware of oil droplets in the gas flows through the piston assembly and crankcase [1–7]. The phenomenon has been generically termed misting, and it has been suggested that misting affects the transport of lubricant through the piston assembly [4, 7], lubricant transport to the combustion chamber [7–9] and lubricant degradation [1, 3, 7, 10]. Lubricant transport to the combustion chamber is understood to affect emissions [7, 11], oil consumption [9, 11, 12] and combustion, particularly via Low-Speed Pre-Ignition (LSPI) [8, 13–16]. LSPI is understood to be a combustion event involving fuel and lubricant droplets [8, 13–18], and is sensitive to lubricant formulation [13, 15, 16, 18, 19]. These droplet flows and their effects are not well understood, so this work aimed to characterise the nature of droplet flows in the engine.

The droplets are thought to be formed by five principal mechanisms, Fig. 1:

1. Vapour Condensation—The volatile fractions of the lubricant that evaporate in the piston assembly may condense if they reach the crankcase, which is significantly cooler [20, 21]. This mechanism is likely to produce aerosol-sized droplets (< 1 µm) [22].
2. Entrainment from Lubricant Film—The high-velocity gas flows moving over an oil film on, for example, the piston lands [9, 23] will cause instabilities in the film

✉ Martin Priest
m.priest@bradford.ac.uk

[1] Formerly of School of Mechanical Engineering, University of Leeds, Leeds, UK

[2] Faculty of Engineering and Informatics, University of Bradford, Bradford, UK

[3] Southwest Research Institute, San Antonio, TX, USA

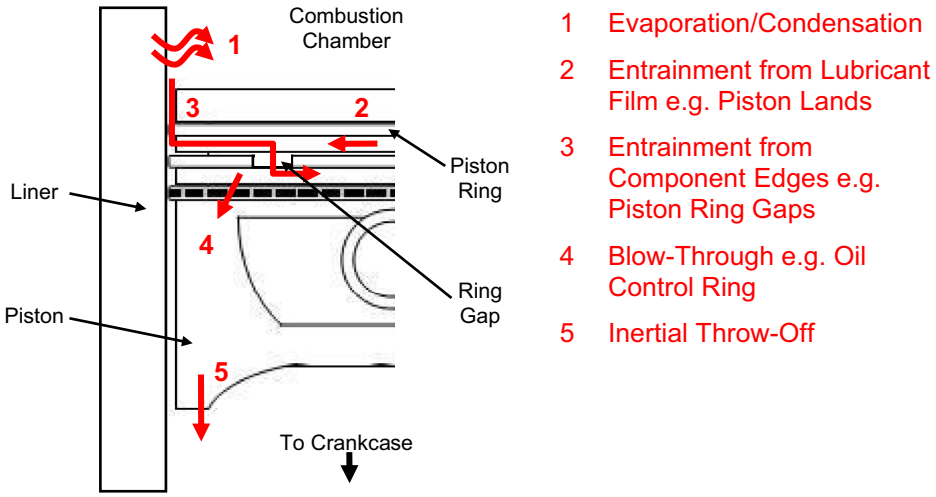

Fig. 1 Lubricant transport mechanisms in the piston assembly of a fired engine

which will entrain droplets. Previous consideration of this mechanism by Gamble et al. [4, 24] showed that this is likely to be present but insignificant.

3. Entrainment from Component Edges—When a high-velocity gas flow encounters an oil film at a component edge at, for example, the piston ring gaps the shear on the lubricant film is greatly increased [25], which may cause droplets to be ripped from the lubricant film [6, 24].
4. Blow-Through—Where a body of lubricant can accumulate in a gas flow path at, for example, the ring–liner interface during bore distortion [26] or in certain designs of oil control ring [27], the pressure differential can cause the body of lubricant to be blown into droplets.
5. Inertial Throw-Off—The movement of lubricant to the edges of rotating or reciprocating components under inertia [9, 23, 28] can cause droplets to be flung from the components [1, 7]. These droplets are thought to be spray-sized (10^2–10^3 µm) [1, 7, 22, 29, 30].

Previous work by the authors has reproduced mechanisms 3 and 4 on a laboratory simulator [31]. This work showed that the simulated droplets contain three characteristic droplet diameters: Mist-sized droplets were found in the ranges < 18 µm and 18–135 µm, termed minor and major, respectively, of which the latter were the most commonly occurring. Spray-sized droplets were seen in the range 135–1000 µm. The proportions of mist and spray droplets varied significantly with oil flow rate. Where the mist-sized droplets were predominant, entrainment at a component edge was the primary mechanism of droplet formation. Where the spray-sized droplets were predominant, blow-through was the primary mechanism. This work also indicated that the viscosity of the lubricant and the molecular structure of viscosity modifiers (VMs) had the greatest effect on the tendency of a lubricant to form droplets. An increase in lubricant viscosity generally decreased the tendency to form mist (entrainment from a component edge) but increased the tendency to form spray (blow-through) [31]. The presence of a viscosity modifier had the same effect as increasing the lubricant viscosity, even between lubricants of equal viscosity. This effect was greater when a high-molecular weight linear polymer was used rather than a high molecular weight star polymer [31].

In this study, a method of measuring the size distribution of droplet flows in the crankcase of a fired engine was developed. This was then used to investigate the effect of varying the viscosity of the lubricant and the concentration of viscosity modifier.

Other published works have studied the presence of droplets in engines. Uy et al. [10] considered the effects of aerosols and filtration on fired diesel engines, measuring droplets/particulates < 1 µm and < 10 µm using electrostatic precipitation: The composition of these droplets/particulates were shown to be soot, wear particles and some components expected in the lubricant—Differences were found between the bulk sump lubricants and the droplets, perhaps suggesting degradation or decomposed lubricant from the piston assembly [32, 33]. Clark and Tatli sampled particulates from the crankcase of a diesel engine, using either a condensator [34], or a electrical mobility particle sizer [35], which were 20–400 nm depending on condition [34, 35]. Johnson et al. sampled droplets generated in either a fired or motored diesel engine using either a high-speed camera [36] or a electrical mobility particle sizer in the range of 5 nm–19 µm [37]. Both droplet number and diameter were shown to be load sensitive: 133 nm was characteristic at low load, 30 nm at high load [37]. Spray-sized droplets were seen to form in the crankcase from rotating components [36]. Behn [38] sampled droplets in the range of 0.1–10 µm through the cylinder wall, where the characteristic diameter was ~ 1 µm and concentration was around 1000 ppm. The concentration of

oil in these droplets was considerably lower than the concentration of fuel. Dollmeyer et al. [39] measured particulates with a characteristic size of 0.3 µm in a diesel engine. However, based on simulation work by the present authors [31], Johnson et al. [36] (who produced droplets with 10 µm and 320–1000 µm characteristic diameters is a rotating atomiser) and Begg et al. [40] (who produced droplets with characteristic diameters between 20-40 µm and up to 120 µm using a scaled, simulated crankcase), droplets with other characteristic diameters are likely to be present in the crankcase too. Wang et al. [41] injected ~ 1-mm-diameter lubricant droplets into a simulated marine engine combustion chamber. These droplets broke up into smaller droplets: in one case, gas flows ripped small droplets from the surface, comparable to the 'rolling' mechanism identified in our previous simulation work [31]; and in another case, larger droplets rapidly disintegrated into smaller droplets. The resulting 'child' droplets were > 40 µm in size.

2 Test Engine

This work was performed on a Ricardo Hydra—a laboratory-based single cylinder, indirect injection, gasoline engine, Fig. 2. The cylinder head is based on a General Motors 2.0 l, 4 cylinder automotive engine. The key properties of this particular version of the Hydra are given in Table 1. The engine is connected to a dynamometer and the engine can be either motored or fired. Several modifications have been previously made to this engine to allow better control and measurement of key tribological parameters: The sump for the crankcase is external to the engine. Thus, the crankcase is nominally dry and a separate lubrication circuit is used for the valve train, which enables lubrication of the crankcase and piston assembly to be studied separately.

Table 1 Performance parameters of the Ricardo hydra engine

Parameter	Condition
Maximum speed	6000 rpm
Maximum torque (Load)	36 Nm
Cylinder bore	86 mm
Piston stroke length	86 mm
Compression ratio	10.5: 1
Fuel	Reference ULG95 Gasoline
Fuel injection	Indirect
Ignition timing	12° Before TDC
Sump volume (external)	3.0 l

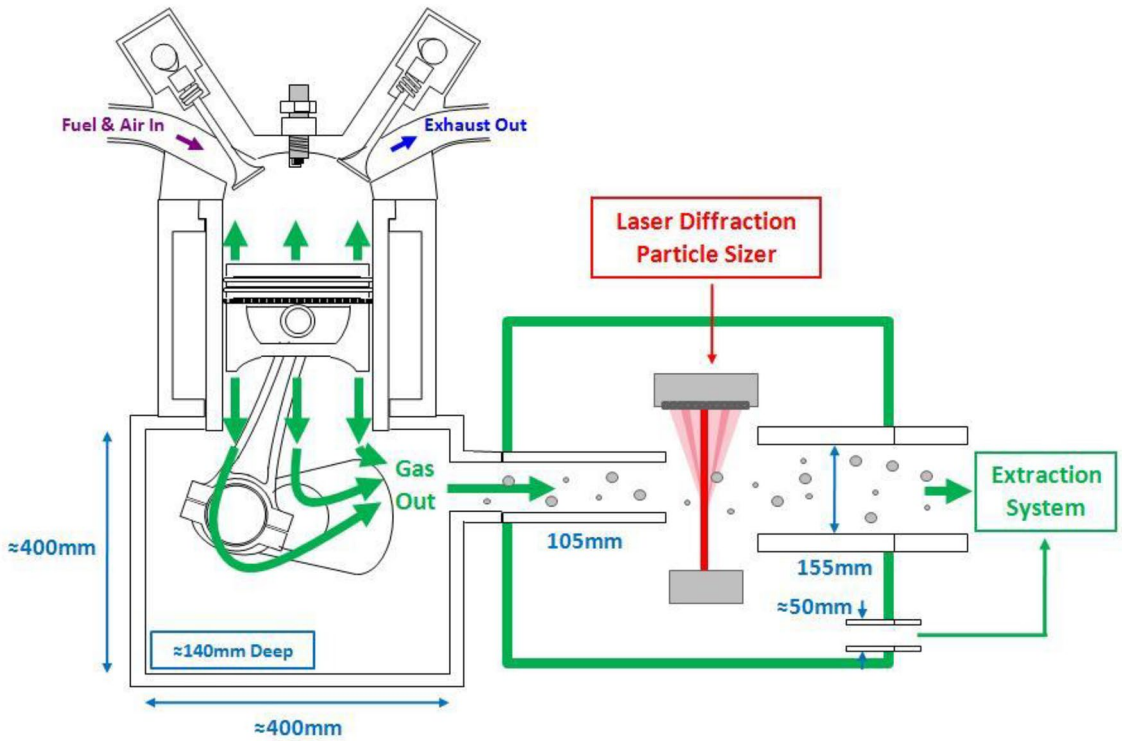

Fig. 2 Schematic of engine mist measurement apparatus

3 Measurement of the Lubricant Droplets in the Crankcase

In previous work [31], representative mist flows were produced in a bespoke laboratory rig and measured in terms of their droplet size distributions and volumetric flow rate using a laser diffraction particle sizer, a Malvern Spraytec 2000. Due to the success of this approach, and in the interests of consistency and validation of the laboratory methodology, the same measurement apparatus was used in this research. The most suitable way to measure the droplets in an engine was to extract gas from the crankcase of the running engine and pass this flow through the beam of the particle sizer, Fig. 2. The gas flow was extracted through a 105-mm-diameter hole in the anti-thrust side wall of the crankcase and passed through a flexible duct into the enclosure that contained the particle sizer. The end of the duct was such that the beam of the particle sizer intersected the centre of the gas flow at the horizontal approximately 60 mm from the outlet, Fig. 3. The gas flow was extracted from the enclosure through a 155-mm-diameter duct that was attached to the extraction system in the engine test cell. The enclosure contained a breather vent to relieve any positive or negative pressure. The extraction system removed gas from the enclosure at a rate of 500 l/min, which is much greater than the blow-by flow from the engine, which, for example, at 1500 rpm, 33% load and 50% throttle is 11.8 l/min (measured using an AVL 442 orifice blow-by flow meter with one damping chamber, Fig. 4). This has two main implications. Firstly, the flow path into the enclosure with the highest flow rate was through the enclosure breather. However, as the blow-by flow is highly pulsatile, the exact flow rate could not be determined. Thus, the flow rate from the crankcase could also not be determined exactly. Whilst it would have been desirable to be able to know the exact flow rate of gas from the crankcase, there were concerns with such a new system about the possibility of concentrating oil droplets and fuel vapour in the proximity of a hot engine and electronic equipment and the potential over-exerting a back-pressure on the crankcase. Thus, the higher than desirable extraction rate was decided upon to prevent these scenarios from occurring.

Secondly, as the exact flow rate from the crankcase could not be determined, the flow rate of the lubricant as droplets could not be determined either. The laser diffraction particle sizer can determine this by deriving a volumetric oil/air ratio from the scattering data and, if the total volumetric flow rate through the detector was known, the oil flow rate could have been calculated.

Therefore, because of these two factors, this investigation focussed on the measurement of the size distributions of the droplet flows in the engine. This was done with reference to the engine speed, load, lubricant base oil viscosity and viscosity modifier concentration. The testing matrix is shown

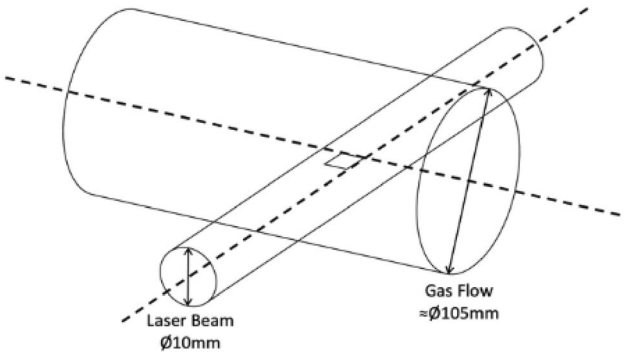

Fig. 3 Intersection of particle sizer beam and gas flow

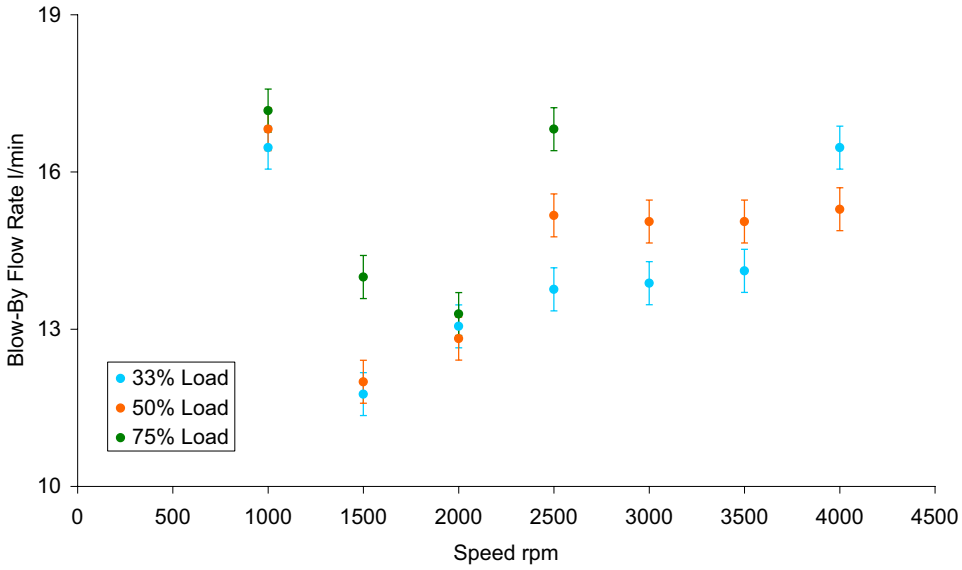

Fig. 4 Blow-by flow rates of Ricardo hydra engine at 50% throttle

in Table 2. Measurements were also taken at an intermediate speed condition of 3200 rpm, but are not reported here due to resonances in the extraction apparatus which caused instability in the readings under these conditions.

The test procedure was designed to produce engine conditions where thermal and tribological equilibrium could be reached, such that the loss of lubricant to the extraction system would not be damaging to the engine or render the results unrepresentative. An abnormal increase in component and coolant temperatures was seen as an indicator of lubricant starvation. The temperatures of the coolant inlet and outlet, the cylinder head and the crankcase were monitored. During all the tests, none of these showed significant variation from normal. Thus, it is concluded that the lubricant supply to the piston assembly was not significantly affected.

The engine was flushed with fresh lubricant before each test. Flushing was performed with a normal crankcase side plate, i.e. without the extraction point. A fresh 3 l sump of the test lubricant was connected, the oil filter changed and the engine was motored for 30 min at 1500 rpm and 50% throttle. After 30 min, another fresh 3 l sump of test lubricant was substituted and motored for a further 30 min under the same conditions. Thus, after a total of an hour, a third sump of fresh test lubricant was connected and the engine run at the test conditions until thermal equilibrium was reached. The engine was then stopped for 5 min, whereupon the side plate was replaced and the engine connected to the measurement and extract apparatus. The engine was then run until the previous thermal equilibrium was reached. When thermal equilibrium was reached, non-droplet-size measurements were recorded as an average over a 30-s period. Droplet size measurements were taken over a 5-min period and averaged. Experiments with variations in sample duration indicated that 5 min gathered sufficient data to dampen variation and that longer sampling periods provided no further improvement in data robustness: The droplet size distribution and oil/air ratio were at a generally steady state from around 2–3 min after the engine reached a constant speed (i.e. before sampling was started), indicating that control over the engine conditions by this method was reasonable. The engine was turned off after 5 min of sampling and allowed to cool before the procedure was restarted.

Previous work on lab-based simulators [22, 31, 42] showed that the lubricant properties that have the greatest effect on the tendency to form droplets were the lubricant viscosity and the presence of polymeric viscosity modifiers in the formulation. Therefore, these two factors were the basis for the lubricant matrix for this series of tests. The test engine was designed for SAE 20 lubricants, so the matrix was based around these: API Group III basestocks were used for their narrower molecular weight distributions compared to Group I and Group II. The matrix is shown in Table 2. Base oils of different viscosity grade were used to evaluate the effect of viscosity (SAE 5, SAE 10 and SAE 20). Different concentrations of a high molecular weight star-type viscosity modifier (VM) were included in an SAE 20 base oil to evaluate the effect of viscosity modifier presence, concentration and blend viscosity. VM contents denote the %wt of VM concentrate i.e. including a diluent oil too. The polymer concentration is proprietary but is within a representative range for a crankcase lubricant. To protect the engine, an overbased calcium sulfonate detergent (1%wt) and a succinimide dispersant (1%wt) were included in all test lubricants.

To aid comparison with the previous work [31], the lubricants investigated here were tested in the laboratory simulator rig used in this work. This rig consisted of a venturi droplet generator that produces flow representative of the flows seen in the piston assembly. The lubricant that did not form droplets and ran out of the system is weighed to determine the proportion of that which does form droplets. The flow rate of droplets formed as a percentage of the total lubricant flow was termed the Droplet Formation Tendency. For a more detailed description of this apparatus, method and interpretation of droplet formation phenomena, see the previous work by the current authors [31]. Figure 5 shows the droplet formation tendency of these lubricants at a range of flow rates. This shows that, at low lubricant flow rates, where greater resistance to droplet formation manifests as lower % Oil Misted, the droplet formation tendency of lubricants without viscosity modifiers was significantly influenced by

Table 2 Test lubricants and conditions for engine misting tests

Base oil			SAE 5	SAE 10	SAE 20	SAE 20	SAE 20	SAE 20
Additives			1% Detergent + 1% Dispersant			5% VM	10% VM	15% VM
η @40 °C mPa.s			18.0	23.2	31.8	50.6	77.8	120.8
Speed	Load	Throttle						
1500	75%	50%						
4500	75%	50%					Repeated	Repeated
4500	50%	50%						Repeated
4500	33%	50%						

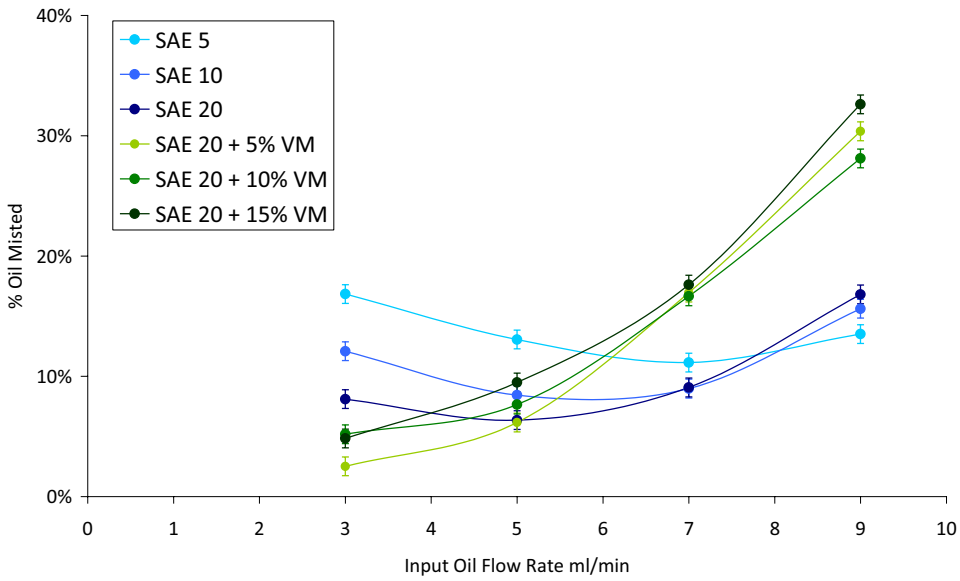

Fig. 5 Laboratory simulator results for misting tendency (% oil misted) of engine test oils

their viscosity: The lower the viscosity, the greater the tendency to produce droplets. Polymer-containing lubricants showed significantly reduced droplet formation tendency. At higher lubricant flow rates, the polymer-containing lubricants showed a more linear increase in droplet formation tendency with flow rate, characteristic behaviour of 'blow-through', where greater resistance to droplet formation under shear causes lubricant to accumulate in the venturi and droplets are formed by air flow through the lubricant rather than over it. Counterintuitively, under these conditions, greater resistance to droplet formation under shear manifests as higher % Oil Misted, i.e. the transition from shear-driven, thin film droplet formation to a bulk flow phenomenon occurs at a lower flow rate. These lubricants had significantly different viscosities but all exhibited similar droplet formation behaviour. This indicated that the droplet formation tendency of these lubricants was most influenced by the presence of polymeric viscosity modifiers and appeared to be independent of polymer concentration in this range. This, in turn, indicated that the increased viscoelasticity imparted by the polymeric viscosity modifiers was the main mechanism. These, therefore, were the properties considered when interpreting the data obtained from the engine.

4 Results

Figure 6 shows the droplet size distributions for polymer-free lubricants at all engine conditions. Based on the repeated tests conducted, the 95% confidence intervals for each of the droplet distribution parameters are shown in Table 3. The statistical significance of all the observations in this work were made with reference to these statistical limits.

As in the laboratory simulation rig, three characteristic droplets diameter ranges were observed in the engine. However, the characteristic diameter ranges were significantly different. These differences in distribution were observed even when comparing the distributions of the same lubricants in both the simulator rig and the engine, Fig. 6, [31]. In the engine, droplet diameters of 0–30 µm characterised the minor misting region, 30–250 µm characterised the major misting region and 250–1000 µm characterised the spray region. In the previous study, the ranges were identified as 0–18 µm, 18–135 µm and 135–1000 µm, respectively [31]. It was observed in Sect. 3 that the presence of detergent and dispersant chosen for this study did not significantly affect the misting properties of the lubricant. So, the likely reasons for the differences in droplet size ranges between the engine and simulator are as follows:

- The simulator reproduced the peak flow through the piston ring gaps. In the engine, the gas velocities will have been lower than this, causing lower shear rates and extension, which could generate larger droplets.
- The lubricant in the engine was at higher temperature. Whilst this meant that lubricant viscosity would be lower (which would normally reduce droplet size) any viscosity modifier molecules will have larger hydrodynamic volume under zero shear conditions. As the VM molecules were star polymers, this may have caused a greater viscoelastic response than at lower temperature. This does not account for the larger droplets using non-VM lubricants, suggesting that the differences in gas velocities was the greater influence.

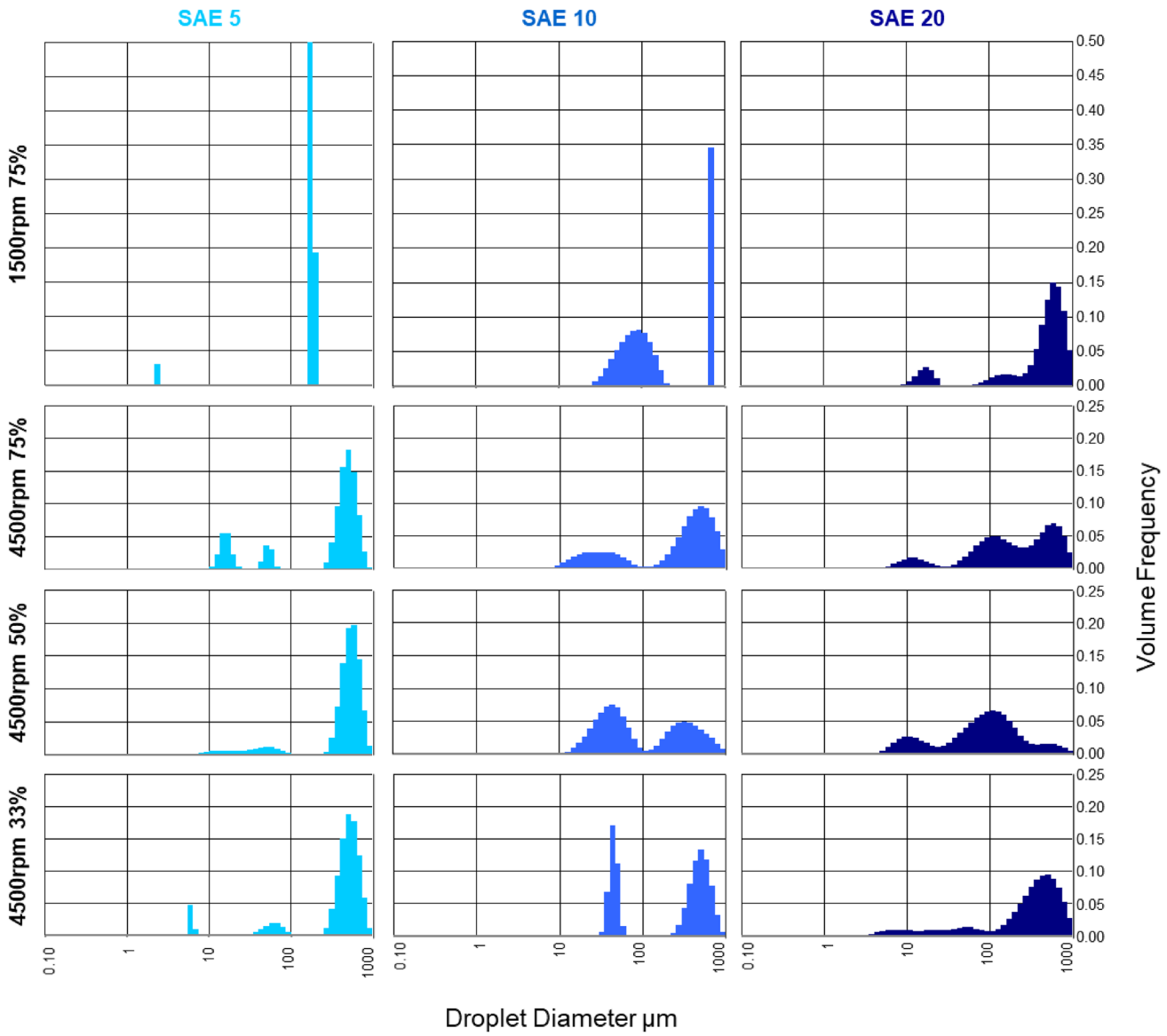

Fig. 6 Droplet size distributions for engine misting tests of lubricants without viscosity modifier

Table 3 95% confidence intervals for droplet size distribution parameters

Characteristic droplet diameter range	95% confidence intervals	
	Mean droplet diameter within range	Relative volumetric proportion of flow in range
Minor Mist = 0.1–30 µm	± 10.8 µm	± 5%
Major Mist = 30–250 µm	± 15 µm	± 8%
Spray = 250–1000 µm	± 63 µm	± 13%

Aerosol-sized droplets (0.1–1.0 µm diameter) were rarely observed in the distributions. They may have been present but were not significant in their volume frequency due to their size. Droplets and particulates in this size range have been identified by other authors [10, 34, 35, 37, 39], albeit using different engines and droplet sizers, and were understood to be formed by the condensation of fuel/oil vapour with or without soot particulates [5, 10, 35], leading to high

concentrations of fuel relative to the rest of the system [38]. Droplets in the 5–15 µm diameter range were more abundant. It is unlikely that the 0.1–1.0-µm-diameter droplets in other studies and the 5–15-µm-diameter droplets here represented the same mechanisms e.g. greater condensation rates in the present study led to a greater droplet diameter. It is more likely that these represented different formation mechanisms. Mist-sized droplets and spray-sized droplets were observed, Fig. 6. The ratios of mist-sized droplets to spray-sized droplets by way of volumetric proportion, indicated by the relative peak heights and areas, were similar to the ratios observed in the laboratory simulator [31].

The measured distributions did not definitively indicate the source mechanism of the droplets in the crankcase. Instead, the distributions appear to be a combination of droplets from different source mechanisms. The trimodal distributions correlate with those formed in the laboratory rig by flow over a component edge. However, some variations in the distributions, as explained below, suggest that some droplets originated elsewhere, e.g. blow-through of oil pockets or inertial throw-off from the con-rod and crankshaft [26, 27, 40].

Mist-sized droplets produced by the SAE 10 lubricant had a unimodal distribution, Fig. 6, but were bimodal for SAE 5 and SAE 20. The root cause was not apparent, although it was repeatable. The distribution for SAE 10 at 4500 rpm and 75% load appeared to show two characteristic sizes with overlapping distributions. However, this did not appear to be the case for the 4500 rpm and 33% load condition. This variation may have been caused by differences in the molecular weight distribution of the base oil, an artefact of the droplet formation process that produced variability in the droplet agglomeration or release from a surface, or a combination of all these.

Therefore, comparisons between lubricants of different viscosity were made between SAE 5 and 10, i.e. bimodal mist-sized droplet distributions: Firstly, at 4500 rpm, the characteristic diameter of the major mist droplets was greater for the higher viscosity lubricant, Table 4. This agrees with Dasch et al. [22] and the laboratory simulator [31], whereby higher viscosity produced larger characteristic droplet sizes. Characteristic diameters of minor mist or spray-sized droplets did not vary significantly. Secondly, the combined volumetric proportion of minor and major mist-sized droplets was lower at 4500 rpm for the lower viscosity lubricant, Table 5. Simulation work measured higher mist-sized droplet proportions with lower viscosity. This was not a contradiction because droplets in the crankcase probably have several source mechanisms, i.e. a lower viscosity lubricant might simultaneously produce a greater quantity of spray-sized droplet by inertial mechanisms, e.g. from the crankshaft [40], reducing the *relative* proportion of mist-sized droplets. Because characteristic diameters (i.e. volume) of major mist droplets were greater with higher viscosity lubricant, but minor mist characteristic diameters were unchanged, the ratio of major to minor mist volumetric proportion was greater with higher lubricant viscosity, Table 6.

With regard to engine conditions, the relative lack of correlation between droplet size distributions for different lubricants at 1500 rpm indicated clear speed dependence of droplet formation. The narrow and relatively non-Gaussian

Table 4 Characteristic droplet sizes for droplet flows extracted from the crankcase under various conditions

Base oil			SAE 5	SAE 10	SAE 20	SAE 20	SAE 20	SAE 20
Additives						5% VM	10% VM	15% VM
			1% Detergent + 1% Dispersant					
η @40 °C mPa.s			18.0	23.2	31.8	50.6	77.8	120.8
Speed	Load	Throttle	Characteristic minor mist diameter µm					
1500	75%	50%	2.4	–	18.5	–	8.0	38.0
4500	75%	50%	18.5	–	12.5	–	9.2	23.0
4500	50%	50%	11.5	–	11.0	9.5	18.5	25.0
4500	33%	50%	6.5	–	8.5	14.0	10.0	15.0
Speed	Load	Throttle	Characteristic Major Mist Diameter µm					
1500	75%	50%	184	100	120	40	60	86
4500	75%	50%	54	38	125	32	54	130
4500	50%	50%	54	47	115	60	73	106
4500	33%	50%	63	47	90	76	74	80
Speed	Load	Throttle	Characteristic Spray Diameter µm					
1500	75%	50%	–	735	630	630	486	630
4500	75%	50%	541	541	630	341	630	–
4500	50%	50%	600	500	541	400	600	547
4500	33%	50%	541	541	541	630	541	630

Table 5 Volumetric proportion of droplets in each characteristic flow extracted from the crankcase under various conditions

Base oil			SAE 5	SAE 10	SAE 20	SAE 20	SAE 20	SAE 20
Additives						5% VM	10% VM	15% VM
			1% Detergent + 1% Dispersant					
η @40 °C mPa.s			18.0	23.2	31.8	50.6	77.8	120.8
Speed	Load	Throttle	Minor Mist Droplets Volumetric Proportion %					
1500	75%	50%	3.2	0.8	11.3	52.4	4.8	1.4
4500	75%	50%	16.4	14.3	10.9	3.7	5.0	5.4
4500	50%	50%	6.2	14.9	21.6	20.7	12.9	0.0
4500	33%	50%	5.8	0.1	11.2	12.1	12.7	3.0
Speed	Load	Throttle	Major Mist Droplets Volumetric Proportion %					
1500	75%	50%	96.8	64.6	11.4	9.9	13.2	9.7
4500	75%	50%	8.6	21.8	44.5	5.9	19.0	94.3
4500	50%	50%	7.5	54.2	65.8	51.8	29.8	17.2
4500	33%	50%	9.0	37.6	23.3	45.6	21.4	41.3
Speed	Load	Throttle	Spray Droplets Volumetric Proportion %					
1500	75%	50%	0.0	34.6	77.3	37.7	82.0	88.9
4500	75%	50%	75.0	63.9	44.5	90.4	76.0	0.3
4500	50%	50%	86.3	30.9	12.6	27.5	57.3	82.8
4500	33%	50%	85.3	62.3	65.5	42.2	65.9	55.7

Table 6 Relative proportion of minor and major mist droplets under various conditions

Base Oil			SAE 5	SAE 10	SAE 20	SAE 20	SAE 20	SAE 20
Additives						5% VM	10% VM	15% VM
			1% Detergent + 1% Dispersant					
η @40 °C mPa.s			18.0	23.2	31.8	50.6	77.8	120.8
Speed	Load	Throttle	Volumetric Proportion Ratio Major Mist: Minor Mist					
1500	75%	50%	30.3	80.8	1.0	0.2	2.8	6.9
4500	75%	50%	0.5	1.5	4.1	1.6	3.8	17.5
4500	50%	50%	1.2	3.6	3.0	2.5	2.3	–
4500	33%	50%	1.6	376.0	2.1	3.8	1.7	13.8

distribution around some characteristic sizes at 1500 rpm could represent either greater uniformity of droplet diameter or a smaller sample size of droplets. At 4500 rpm, droplet size distributions showed little significant variation with load. However, one statistically significant observation was that characteristic diameters of minor mist droplets increased at higher loads, when such droplets were present. Droplets may have grown by condensation of fuel/oil vapour: Higher piston assembly temperatures at higher loads increased evaporation rate, and greater temperature difference between piston assembly and sump increased condensation rate. Minor mist droplets will have been most greatly affected by condensation due to high surface-area-to-volume ratio.

Figure 7 shows the variation in droplet size distribution for lubricants containing varying concentrations of viscosity modifier. Because the viscosity modifier was added to the same SAE 20 base oil, there were no lubricants with the same dynamic or kinematic viscosity at either crankcase (~ 60 °C) or piston assembly temperature (> 100 °C [43]). Overall, the proportion of mist-sized droplets was lower when viscosity modifier was present. This effect was significant at 10% and 15% but marginal at 5% concentration, especially at low load. This could represent a reduction in mist formation or an increase in spray, perhaps both.

Considering engine conditions: The proportion of mist was significantly lower at 75% load than at 33–50%, Table 5. Within this, major mist proportion at 50% load was lower than at 33% load, most clearly with 10–15% VM concentration, but was insignificantly different at 75%. Referring to Fig. 5 (where laboratory scale testing indicated primarily viscosity-dependent droplet formation in non-VM lubricants, and primarily viscoelasticity-defined droplet formation in VM-containing lubricants): Because non-VM lubricants did not show this load dependence, it suggests that the load-dependent differences in droplet formation with VM-containing lubricants in the engine are a viscoelastic effect. Perhaps the higher piston assembly temperatures at 50–75% load increased the viscoelastic reduction in droplet

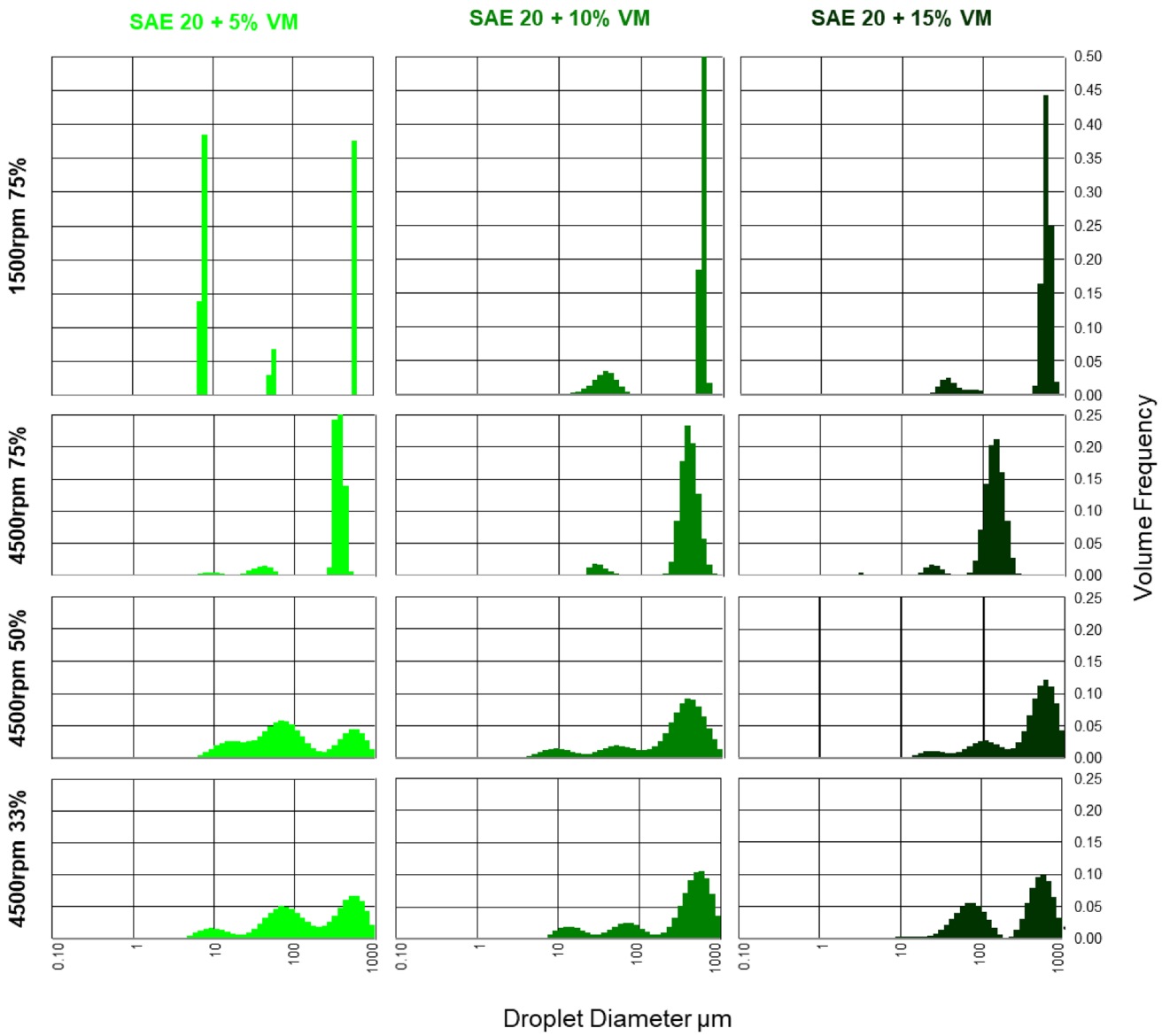

Fig. 7 Droplet size distributions for engine misting tests of lubricants containing viscosity modifier

formation, i.e. when polymer molecules extended. This effect may not have been as great at 5% VM due to reduced total capacity for viscoelastic energy storage. There were greater similarities in the droplet distributions between 1500 and 4500 rpm conditions. However, the only statistically significant change was higher characteristic diameter spray droplets at 1500 rpm: These correspond more closely to spray droplets at 33% load, i.e. lower temperatures and gas flow rates. Overall, characteristic droplet diameter peaks showed lower variation around the mean at 1500 rpm.

There were extremely low proportions of minor mist proportions at 75% load, at both 1500 rpm and 4500 rpm: The proportion was higher in lubricants without VMs, suggesting a viscoelastic effect. However, minor mist proportions were greater for the same lubricant at 33–50% load, i.e. VM was not the only factor. Perhaps viscoelasticity affected particular flow mechanisms that were more influential at higher load. Unlike with non-VM oils, there was no significant change in these droplet diameters with load. Major mist droplets at 75% load had smaller characteristic diameters than at 33–50% load. This was more pronounced at 4500 rpm than 1500 rpm. This change was only observed for lubricants containing VM: Characteristic major mist diameters for SAE 20 base oil containing 5% and 10% VM were smaller than for SAE 20 base oil alone, Table 4.

Greater VM concentrations had progressively greater effect, but not linear. A minimum VM concentration appeared to be needed to affect different droplet formation

mechanisms. At 75% load, this appeared to be between 5 and 10% VM. At 33–50% load, this appeared to be between 10 and 15%; for example, suppression or elimination of minor mist droplets was seen for 10% VM at 75% load but for 15% VM at 33% and 75% load.

5 Droplet Stability and Breakup

After lubricant droplets are formed, they continue to interact with the gas flows in which they are entrained. Droplets can deform and break up into smaller droplets and/or coalesce into larger droplets as they interact with each other. Two key parameters were used to describe droplet stability: Firstly, the Weber Number [44]:

$$We = \frac{\rho_G v^2 d}{\sigma}, \tag{1}$$

where ρ_G is the density of the gas phase, v is the relative velocity between the droplet and the gas flow around it, d is the diameter of the droplet and σ is the surface tension of the droplet. This is the ratio of surface tension forces to the inertial forces. *We* is considered the most influential descriptive parameter for droplet breakup, even in combination with other parameters [45].

Secondly, the Ohnesorge Number [44]:

$$Oh = \frac{\eta_L}{\sqrt{\rho_L \sigma d}}, \tag{2}$$

where ρ_L is the density of the droplet liquid. This is the ratio of viscous forces to the surface tension forces. When *Oh* is greater than 1, the viscosity of the droplet is considered to have the dominant effect over the droplet breakup process.

Different droplet breakup mechanisms have been observed:

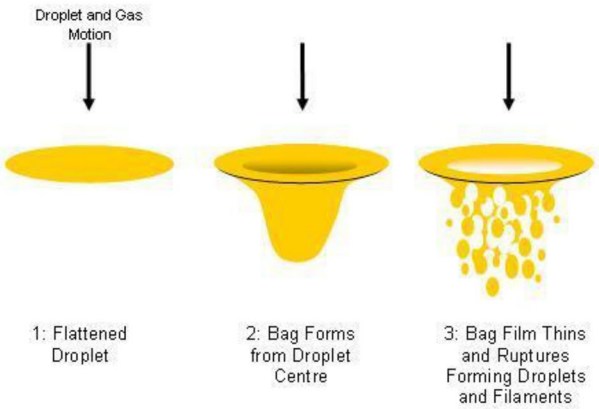

Fig. 8 Schematic of droplet bag breakup

- **Bag Breakup**, Fig. 8.
- **Shear Breakup**, Fig. 9. This mechanism may be similar to that observed by Wang et al. [41].
- **Catastrophic Breakup**. The large drag-induced pressure and shear acting on the droplet causes the almost instantaneous destruction of the droplet into small 'child' droplets, Fig. 10.

Table 7 shows various models and the dimensionless parameters that describe the transitions between these mechanisms. The Cascade Atomisation and Breakup [46] model was selected for this study because it covers all three breakup mechanisms and was validated against non-evaporating fluids.

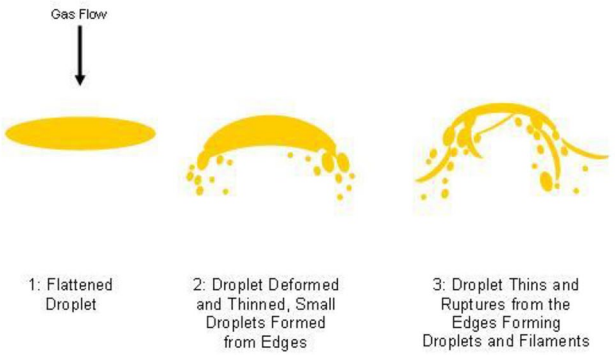

Fig. 9 Schematic of droplet shear breakup

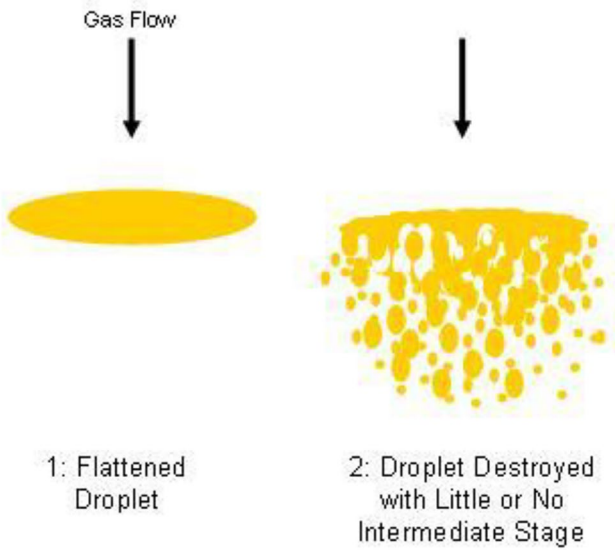

Fig. 10 Schematic of droplet catastrophic breakup

Table 7 Transitions between droplet breakup mechanisms by dimensionless parameters: *Re* is the Reynold's number of the droplet-gas flow [44]

Model	Reitz and Diwakar	Taylor Analogy Breakup	Cascade Atomisation and Breakup	Jeng and Deng		Arcoumanis et al. 1997
Reference	[48]	[45]	[46]	[45]		[49]
Parameter				We	$WeRe^{-0.5}$	
Bag Breakup	$We > 6$	–	$We > 5$	8–40	0.2–1.6	$We > 12$
Shear Breakup	$WeRe^{-0.5} > 0.5$	$We > 80$	$We > 80$	20–20,000	1–20	$We > 100$
Catastrophic Breakup	–	–	$We > 350$	2000–200,000	20–200	$We > 350$

The following generalised flows were considered and the assumed conditions are shown in Table 8:

- **Crankcase at typical big-end bearing oil temperature (100 °C):** Representing droplets formed from the crank assembly. Pressure and gas properties were calculated from the Ideal Gas Laws and the measured crankcase pressure for each individual test. The droplet velocity range of 5-20 ms^{-1} was applied, as measured by Begg et al. [40]. Linear velocities of the crank counterweight tips were similar: 20 ms^{-1} @1500 rpm and 59 ms^{-1} @4500 rpm for the Ricardo Hydra, 21 ms^{-1} @3000 rpm and 42 ms^{-1} @6000 rpm for Begg et al. [40]).
- **Crankcase at typical gas temperature (measured by crankcase oil sensor: 40–70 °C for this engine).** Gas flow conditions were as above but oil temperature was assumed equal to surrounding gas flow.
- **Piston assembly at the second land**. Considering that major mist and minor mist droplets could be produced in the piston assembly, conditions were calculated from Gamble [4] who modelled this engine at 2500 rpm, 50% load and 50% throttle. Therefore, as these were not the exact operating conditions here, this is intended only as an exploratory parametric estimate from the best available information and a basis for further investigation. The characteristic velocity was the peak velocity through the piston second land. The minimum (68 ms^{-1}) was when the top ring gap was at the anti-thrust side of the piston and the land area was largest. The maximum (145 ms^{-1}) when the top ring gas was near the thrust side of the piston and the land area was smallest. Spray was ignored as typical droplet diameters were comparable to the piston ring gap (fitted gap = 0.603 mm).

Cascade Breakup Model criteria were applied to droplets with the mean droplet diameter in each characteristic droplet diameter range as defined above: Minor Mist = 0.1–30 µm, Major Mist = 30–250 µm and Spray = 250–1000 µm.

Table 9 shows the outcomes of the Cascade Breakup model applied to the crankcase. Table 10 shows the outcomes of the Cascade Breakup model for the piston assembly. In the crankcase, under both conditions, breakup of spray droplets would occur at relative gas-droplet velocity of approximately 17 ms^{-1}. The Weber number of these flows implies that these droplets would be in the bag breakup regime. At the 100 °C condition, spray Ohnesorge Number was 0.03–0.15, i.e. greater dependence on surface tension than viscosity. Conversely, at local gas temperature, spray Ohnesorge Number was 3.1–18.2, i.e. high dependence on viscosity. Detailed thermodynamic analysis would be required to determine the characteristic condition. Under all crankcase conditions, the major mist and minor mist droplets would not readily break up. Changes to these droplets would occur by any coalescence, deposition or condensation. Latter mechanisms aside, droplet from the crankcase would not be significantly changed during extraction and measurement.

Crankcase conditions did not vary greatly with load, so the greatest cause of changes in breakup parameters was variation in droplet size diameter, i.e. engine conditions

Table 8 Gas and lubricant properties in the piston assembly and crankcase of test engine, as applied to droplets in breakup models

Parameter	Crankcase (100 °C)	Crankcase (Gas Temp)	Piston Assembly
Local Gas Temperature (K)	310–340	310–340	423
Gas Density at Maximum Local Pressure (kg/m^3)	1.02–1.12	1.02–1.12	8.40
Characteristic Velocity (ms^{-1})	5–20	5–20	68–145
Lubricant Dynamic Viscosity at Local Temperature ($mPa.s$)	3.7–17.0	11.6–65.8	≈ 1.0
Lubricant Density at Local Temperature (kg/m^3)	780–800	800–820	750–770

Table 9 Droplet breakup parameters for droplets under crankcase conditions

Weber Number

We is independent of oil viscosity and density. Values apply for both 100°C and Local Gas T Condition

	Speed	Load	Throttle	v = 5 ms^{-1} SAE 5	SAE 10	SAE 20	SAE 20 + 5% VM	SAE 20 + 10% VM	SAE 20 + 15% VM	v = 10 ms^{-1} SAE 5	SAE 10	SAE 20	SAE 20 + 5% VM	SAE 20 + 10% VM	SAE 20 + 15% VM	v = 15 ms^{-1} SAE 5	SAE 10	SAE 20	SAE 20 + 5% VM	SAE 20 + 10% VM	SAE 20 + 15% VM	v = 16 ms^{-1} SAE 5	SAE 10	SAE 20	SAE 20 + 5% VM	SAE 20 + 10% VM	SAE 20 + 15% VM
Minor Mist	1500	75%	50%	0.002	-	0.02	-	0.01	0.04	0.01	-	0.07	-	0.03	0.14	0.02	-	0.15	-	0.06	0.32						
	4500	75%	50%	0.02	-	0.01	-	0.01	0.02	0.06	-	0.04	-	0.03	0.08	0.14	-	0.10	-	0.07	0.18						
	4500	50%	50%	0.01	-	0.01	0.01	0.02	0.02	0.04	-	0.04	0.03	0.06	0.09	0.09	-	0.09	0.07	0.14	0.19						
	4500	33%	50%	0.01	-	0.01	0.01	0.01	0.01	0.02	-	0.03	0.05	0.04	0.05	0.05	-	0.07	0.11	0.08	0.12						
Major Mist	1500	75%	50%	0.17	0.09	0.11	0.04	0.05	0.08	0.69	0.37	0.42	0.14	0.22	0.32	1.55	0.82	0.95	0.32	0.48	0.72						
	4500	75%	50%	0.05	0.03	0.11	0.03	0.05	0.11	0.18	0.13	0.43	0.11	0.18	0.44	0.42	0.29	0.96	0.25	0.41	0.99						
	4500	50%	50%	0.05	0.04	0.10	0.05	0.06	0.09	0.19	0.16	0.40	0.21	0.25	0.36	0.42	0.36	0.90	0.47	0.57	0.82						
	4500	33%	50%	0.06	0.04	0.08	0.07	0.07	0.07	0.22	0.16	0.32	0.26	0.26	0.28	0.50	0.36	0.71	0.59	0.59	0.63						
Spray	1500	75%	50%	-	0.7	0.6	0.6	0.4	0.6	-	2.7	2.2	2.2	1.7	2.3	-	6.1	5.0	5.0	3.9	5.3	-	6.9	5.7	5.7	4.5	6.0
	4500	75%	50%	0.5	0.5	0.5	0.3	0.5	-	1.9	1.8	2.2	1.2	2.1	-	4.2	4.1	4.8	2.6	4.8	-	4.7	4.7	5.5	3.0	5.5	-
	4500	50%	50%	0.5	0.4	0.5	0.3	0.5	0.5	2.1	1.7	1.9	1.4	2.1	1.9	4.7	3.9	4.2	3.1	4.7	4.2	5.3	4.4	4.8	3.6	5.3	4.8
	4500	33%	50%	0.5	0.5	0.5	0.5	0.5	0.5	1.9	1.9	1.9	2.2	1.9	2.2	4.3	4.2	4.3	4.9	4.3	4.9	4.9	4.8	4.8	5.6	4.9	5.6

	Speed	Load	Throttle	v = 17 ms^{-1} SAE 5	SAE 10	SAE 20	SAE 20 + 5% VM	SAE 20 + 10% VM	SAE 20 + 15% VM	v = 18 ms^{-1} SAE 5	SAE 10	SAE 20	SAE 20 + 5% VM	SAE 20 + 10% VM	SAE 20 + 15% VM	v = 19 ms^{-1} SAE 5	SAE 10	SAE 20	SAE 20 + 5% VM	SAE 20 + 10% VM	SAE 20 + 15% VM	v = 20 ms^{-1} SAE 5	SAE 10	SAE 20	SAE 20 + 5% VM	SAE 20 + 10% VM	SAE 20 + 15% VM
Minor Mist	1500	75%	50%																			0.04	-	0.26	-	0.11	0.56
	4500	75%	50%																			0.25	-	0.17	-	0.12	0.31
	4500	50%	50%																			0.16	-	0.15	0.13	0.26	0.34
	4500	33%	50%																			0.09	-	0.12	0.19	0.14	0.21
Major Mist	1500	75%	50%																			2.75	1.46	1.70	0.56	0.86	1.27
	4500	75%	50%																			0.74	0.52	1.71	0.44	0.73	1.76
	4500	50%	50%																			0.75	0.64	1.59	0.83	1.01	1.45
	4500	33%	50%																			0.90	0.65	1.26	1.05	1.05	1.12
Spray	1500	75%	50%	-	10.8	8.9	8.9	7.0	9.3	-	8.7	7.2	7.2	5.6	7.6	-	9.7	8.0	8.0	6.3	8.4	-	10.8	8.9	8.9	7.0	9.3
	4500	75%	50%	7.4	7.3	8.6	4.7	8.5	-	6.0	5.9	7.0	3.8	6.9	-	6.7	6.6	7.8	4.3	7.7	-	7.4	7.3	8.6	4.7	8.5	-
	4500	50%	50%	8.3	6.9	7.5	5.6	8.3	7.5	6.7	5.6	6.1	4.5	6.8	6.1	7.5	6.3	6.8	5.0	7.5	6.8	8.3	6.9	7.5	5.6	8.3	7.5
	4500	33%	50%	7.7	7.5	7.6	8.7	7.7	8.8	6.2	6.1	6.1	7.1	6.3	7.1	6.9	6.8	6.8	7.9	7.0	7.9	7.7	7.5	7.6	8.7	7.7	8.8

Ohnesorge Number

Oh is independent of v

	Speed	Load	Throttle	Oil at 100°C SAE 5	SAE 10	SAE 20	SAE 20 + 5% VM	SAE 20 + 10% VM	SAE 20 + 15% VM	Oil at Local Gas Temperature SAE 5	SAE 10	SAE 20	SAE 20 + 5% VM	SAE 20 + 10% VM	SAE 20 + 15% VM
Minor Mist	1500	75%	50%	15.4	-	8.1	-	26.7	17.8	48.3	-	28.1	-	101.8	68.9
	4500	75%	50%	5.6	-	9.9	-	24.9	22.9	17.4	-	34.1	-	94.9	88.6
	4500	50%	50%	7.0	-	10.5	17.0	17.6	21.9	22.1	-	36.4	60.9	66.9	84.9
	4500	33%	50%	9.4	-	12.0	14.0	23.9	28.3	29.4	-	41.4	50.2	91.0	109.7
Major Mist	1500	75%	50%	1.8	2.8	3.2	8.3	9.8	11.8	5.5	9.2	11.0	29.8	37.2	45.9
	4500	75%	50%	3.3	4.6	3.1	9.2	10.3	9.6	10.2	15.0	10.8	33.2	39.2	37.3
	4500	50%	50%	3.3	4.2	3.3	6.8	8.9	10.7	10.2	13.5	11.3	24.3	33.8	41.3
	4500	33%	50%	3.0	4.2	3.7	6.0	8.8	12.3	9.4	13.5	12.7	21.5	33.6	47.5
Spray	1500	75%	50%	-	0.03	0.04	0.07	0.11	0.14	-	3.4	4.8	7.5	13.1	16.9
	4500	75%	50%	0.03	0.04	0.04	0.09	0.10	-	3.2	4.0	4.8	10.2	11.5	-
	4500	50%	50%	0.03	0.04	0.05	0.08	0.10	0.15	3.1	4.1	5.2	9.4	11.8	18.2
	4500	33%	50%	0.03	0.04	0.05	0.07	0.10	0.14	3.2	4.0	5.2	7.5	12.4	16.9

Table 10 Droplet breakup parameters for droplets under piston assembly conditions

Weber Number

	Speed	Load	Throttle	v = 68 ms^{-1} SAE 5	SAE 10	SAE 20	SAE 20 + 5% VM	SAE 20 + 10% VM	SAE 20 + 15% VM	v = 145 ms^{-1} SAE 5	SAE 10	SAE 20	SAE 20 + 5% VM	SAE 20 + 10% VM	SAE 20 + 15% VM
Minor Mist	1500	75%	50%	3	-	24	-	10	49	14	-	109	-	47	224
	4500	75%	50%	24	-	16	-	12	30	109	-	74	-	54	135
	4500	50%	50%	15	-	14	12	24	32	68	-	65	56	109	147
	4500	33%	50%	8	-	11	18	13	19	38	-	50	82	59	88
Major Mist	1500	75%	50%	238	129	155	52	78	111	1083	589	706	234	353	505
	4500	75%	50%	70	49	162	41	70	168	318	224	736	188	318	765
	4500	50%	50%	70	60	149	78	94	137	318	274	677	353	427	623
	4500	33%	50%	82	60	116	98	95	104	371	274	530	447	433	471

Ohnesorge Number

	Speed	Load	Throttle	v = 68 ms^{-1} SAE 5	SAE 10	SAE 20	SAE 20 + 5% VM	SAE 20 + 10% VM	SAE 20 + 15% VM	v = 145 ms^{-1} SAE 5	SAE 10	SAE 20	SAE 20 + 5% VM	SAE 20 + 10% VM	SAE 20 + 15% VM
Minor Mist	1500	75%	50%	4.2	-	1.5	-	2.3	1.0	4.2	-	1.5	-	2.3	1.0
	4500	75%	50%	1.5	-	1.8	-	2.1	1.3	1.5	-	1.8	-	2.1	1.3
	4500	50%	50%	1.9	-	1.9	2.1	1.5	1.3	1.9	-	1.9	2.1	1.5	1.3
	4500	33%	50%	2.5	-	2.2	1.7	2.0	1.7	2.5	-	2.2	1.7	2.0	1.7
Major Mist	1500	75%	50%	0.48	0.65	0.59	1.02	0.83	0.70	0.48	0.65	0.59	1.02	0.83	0.70
	4500	75%	50%	0.88	1.05	0.58	1.14	0.88	0.57	0.88	1.05	0.58	1.14	0.88	0.57
	4500	50%	50%	0.88	0.95	0.60	0.83	0.76	0.63	0.88	0.95	0.60	0.83	0.76	0.63
	4500	33%	50%	0.81	0.95	0.68	0.74	0.75	0.72	0.81	0.95	0.68	0.74	0.75	0.72

influence indirectly by affecting droplet size. For instance, at 1500 rpm and 75% load, the SAE 10 and SAE 20 droplets would break up at around 15 ms^{-1}, due to their larger initial diameter. 5% VM lubricant at 4500 rpm and at 75% load was the only condition where droplet diameter affected the transition to breakup, where smaller characteristic diameters would make droplets stable up to 20 ms^{-1}.

Comparing the major mist droplets of the SAE 20 and SAE 20 + 5% VM at hypothetical 100 °C conditions, the presence of VM increased the Ohnesorge Number [44] by

62% at 33% load and 196% at 75% load. A change of similar magnitude would also be seen at the crankcase local temperature condition. This represents the largest difference in Ohnesorge Number between any of the evaluated conditions. Thus, there would be a large difference in the viscosity-dependent behaviour of the droplets formed by these two lubricants. This further suggests that there was change in the balance of the droplet formation mechanisms caused by the presence of VM.

In the piston assembly, minor mist Ohnesorge Numbers under all conditions were greater than 1, implying high viscosity dependence. However, major mist flows had $Oh = 0.5–1.1$, i.e. significantly lower viscosity dependence. Minor and major mist droplets at both conditions (68 ms^{-1} and 145 ms^{-1}) would be expected to break up readily. Minor mist droplets at 68 ms^{-1} would be in the bag breakup regime and many major mist droplets at 145 ms^{-1} would be in the catastrophic breakup regime. Minor mist droplets at 145 ms^{-1} and major mist droplets at 68 ms^{-1} were in either the bag or shear regime depending on original size, but are close to the transition *We* of 80. Essentially, droplets would quickly break up in the piston assembly. This may increase lubricant evaporation from smaller droplets with their higher surface-area-to-volume ratio.

6 Comparison with Laboratory Simulator

Comparing measurements from the laboratory simulator [31] and the engine:

- Bimodal and trimodal droplet size distributions from the simulator were similar in form to distributions from the engine, albeit with different characteristic size ranges.
- The characteristic droplet sizes in the engine were significantly larger than the comparable ranges in the laboratory simulator. The cause of this could be temperature- or flow velocity-dependent.
- The simulator reproduced the peak flow velocities in the piston ring gaps. In the engine, flow velocities vary through the engine cycle, and droplets are formed in other locations where velocities are lower (e.g. crankshaft, oil control ring). Lower velocity flows have lower Reynolds' (*Re*) and Weber Numbers, and would exert lower shear stresses on the lubricant. This could cause larger droplets to form.
- Higher temperatures in the engine will have reduced the lubricant viscosity, which will have increased *Re* and *We*. However, higher lubricant temperatures will have also increased the low shear size of the VM molecules: As VMs were star polymers, greater molecular size will have reduced the capacity for each arm to extend, but will have increased the radius of gyration i.e. the volume of lubricant influenced by the polymer molecule, which may increase viscoelasticity. Further work is needed to elucidate these mechanisms.
- The simulator operated at a single temperature. In the engine, droplet distributions showed some temperature dependence.
- In the simulator, the influence of star polymers on droplet formation was concentration-dependent. In the engine, some concentration dependence was observed but was not linear or uniform, reflecting that distributions contained droplets from different source mechanisms.
- In both the simulator and the engine, the lubricant viscosity and the presence of viscosity modifier influenced the droplet formation.
- Overall, the simulator reproduced many of the phenomena observed in the engine. With the current equipment, the simulator was able to measure 'droplet formation tendency' but this could not be measured in the engine.

7 Implications for Engines

These findings have implications for engine tribology:

- To reduce friction power loss, there is a trend for progressively lower viscosity crankcase lubricants. This could form smaller lubricant droplets and a greater proportion of minor mist-sized droplets. Minor mist droplets are likely to have longer residence times in gas flows. This could lead to a greater flow rate of lubricant through breathers, into exhaust recirculation systems and turbochargers, where varnish and deposit can be formed [10].
- Droplets in the piston assembly area have low stability and should readily break up. This will have implications for Low-Speed Pre-Ignition (LSPI), where lubricant droplets and lubricant composition are key factors [8, 13–16].
- Hybrid engines undergo more transient phenomena during start-stop, including starting at high speeds [47]. Transient events have been shown to contribute to blow-through of oil pockets in the piston assembly [27], which will could increase sensitivity to droplet formation and viscometrics.
- If reduced lubricant viscosity leads to reduced droplet size in the major mist region and greater formation of minor mist droplets leading, the specific surface area lubricant will increase. This may increase the degradation rate and evaporation rate of the lubricant.
- The predicted short lifetime of droplets in the piston assembly could increase the rate of transfer from liquid lubricant film to vapour in the gas flows in this region if lubricant viscosity is reduced.

- The presence of VM reduced the formation of minor mist droplets and major mist droplets, but effects have some concentration dependency. Formulators should consider the type and concentration of VM, and the parameters they affect [31].

8 Conclusions

Lubricant droplet flows in the crankcase of a fired gasoline engine have been extracted and droplet size distributions measured:

- Three characteristic droplet size regions were identified: Spray sized (250–1000 µm); Major mist (30–250 µm); and Minor mist (0.1–30 µm).
- Mist-sized droplets in the crankcase would stable under all measured conditions, though spray-sized droplets would break up at a characteristic speed ~ 17 ms^{-1}. Droplets of all sizes in the piston assembly were predicted to break up into small droplets.
- In lubricants without VM, higher base oil viscosity generated a lower relative proportion of mist droplets, especially minor mist droplets, and major mist droplets had larger characteristic diameter.
- The presence of VM reduced the proportion of mist droplets, especially at high load. Minor mist droplets were greatly reduced or completely suppressed. This was understood to be an effect of the viscoelasticity contributed by the VM, as this appears more influential on lubricant droplet formation than other properties, and correlates with the reduction in mist-sized droplets with VM observed on a laboratory scale [31]
- Higher VM concentration had progressively greater effect. However, this was not linear as droplet size distributions were the cumulative product of several mechanisms, i.e. VM affected different mechanisms to varying extents.
- These findings validate and contextualise previous work performed on a laboratory simulator rig.

Acknowledgements Many thanks to the EPSRC Equipment Loan Pool for access to the laser diffraction particle sizer. The authors also wish to acknowledge the expert suggestions and feedback from Professor R C Coy whilst he was a visiting professor at the University of Leeds, UK

Author Contributions All authors contributed to the design of experiments, the execution and analysis of the experiments, and the writing/reviewing of the manuscript.

Data Availability For information about the availability of the data used in this study, please contact the corresponding author.

Declarations

Conflict of interest The authors declare no competing interests.

References

1. Burnett, P.J.: SAE Technical Paper 920089 (1992).
2. Cho, Y., Tian, T.: Modeling engine oil vaporization and transport of the oil vapor in the piston ring pack of internal combustion engines. *SAE Technical Paper 2004-01-2912* (2004).
3. DePetris, C., Giglio, V., Police, G.: SAE Technical Paper 961216 (1996).
4. Gamble, R.J.: PhD Thesis, University of Leeds, UK (2003).
5. Hare, C.T., Baines, T.M.: Characterization of diesel crankcase emission. *SAE Technical Paper 770719* (1977).
6. Thirouard, B., Tian, T., Hart, D.P.: Investigation of oil transport mechanisms in the piston ring pack of a single cylinder diesel engine, using two dimensional laser induced fluorescence. *SAE Technical Paper 982658* (1998).
7. Yilmaz, E., Tian, T., Wong, V.W., Heywood, J.B.: The contribution of different oil consumption sources to total oil consumption in a spark ignition engine. *SAE Technical Paper 2004-01-2909* (2004).
8. Dahnz, C., Han, K.-M., Spicher, U., Magar, M., Schiessl, R., Maas, U.: Investigations on pre-ignition in highly supercharged SI engines. *SAE Technical Paper 2010-01-0355* (2010).
9. Veettil, M. P., Shi, F.: CFD analysis of oil/gas flow in piston ring pack. *SAE Technical Paper 2011-01-1406* (2011).
10. Uy, D., Storey, J., Sluder, C. S., Barone, T., Lewis, S., Jagner, M.: Effects of oil formulation, oil separator, and engine speed and load on the particle size, chemistry, and morphology of diesel crankcase aerosols. *SAE Technical Paper 2016-01-0897* 2016.
11. SAE, J2794 Power cylinder oil consumption: transport mechanisms (2007).
12. Ito, A., Tsuchihashi, K., Nakamura, M.: A Study on the mechanism of engine oil consumption—oil upwards transport via piston oil ring gap. *SAE Technical Paper 2011-01-1402* (2011).
13. Fletcher, K.A., Dingwell, L., Yang, K., Lam, W.Y., Styer, J.P.: Engine oil additive impacts on low speed pre-ignition. *SAE Technical Paper 2016-01-2277* (2016).
14. Hu, T., Teng, H., Luo, X., Lu, C., Luo, J.: Influence of fuel dilution of crankcase oil on ignitability of oil particles in a highly boosted gasoline direct injection engine. *SAE Technical Paper 2015-01-2811* (2015).
15. Kassai, M., Torii, K., Shiraishi, T., Nada, T., Goh, T.K., Wilbrand, K., Wakefield, S., Healy, A., Doyle, D., Cracknell, R., Shibuya, M.: Research on the effect of lubricant oil and fuel properties on LSPI occurrence in boosted S.I. engines. *SAE Technical Paper 2016-01-2292* (2016).

16. Ritchie, A., Boese, D., Young, A. W.: Controlling low-speed pre-ignition in modern automotive equipment part 3: identification of key additive component types and other lubricant composition effects on low-speed pre-ignition. *SAE Technical Paper 2016-01–0717* (2016).
17. Gupta, A., Shao, H., Remias, J., Roos, J., Wang, Y., Long, Y., Wang, Z., Shuai, S.-J.: Relative impact of chemical and physical properties of the oil-fuel droplet on pre-ignition and superknock in turbocharged gasoline engines. *SAE Technical Paper 2016-01-2278* (2016).
18. Kassai, M., Shiraishi, T., Noda, T., Hirabe, M., Wakabayashi, Y., Kusaka, J., Daisho, Y.: An investigation on the ignition characteristics of lubricant component containing fuel droplets using rapid compression and expansion machine. *SAE Technical Paper 2016-01–2168* (2016).
19. Mayer, M., Hofmann, P., Geringer, B., Williams, J., Moss, J., Kapus, P.: Influence of different oil properties on low-speed preignition in turbocharded direct in jection spark ignition engines. *SAE Technical Paper 2016-01-0718* (2016).
20. Taylor, R.I., Evans, P.G.: In-situ piston measurements. Proc IMechE: J J Eng Tribol **218**, 185–200 (2004)
21. Yilmaz, E., Tian, T., Wong, V. W., Heywood, J. B.: An experimental and theoretical study of the contribution of oil evaporation to oil consumption. *SAE Technical Paper 2002-01-2684* (2002).
22. Dasch, J.M., D'Arcy, J.B., Kinare, S.S., Yin, Y., Kopple, R.G., Salmon, S.C.: Mist generation from high-speed grinding with straight oils. Tribol. Trans. **51**, 381–388 (2008)
23. Bregar, J., Rienacker, A., Gohl, M., Knoll, G.: Fuel transport across the piston ring pack: development of a computationally efficient simulation model. *SAE Technical Paper 2015-01-2534* (2015).
24. Gamble, R.J., Priest, M., Taylor, C.M.: Detailed analysis of oil transport in the piston assembly of a gasoline engine. Tribol. Lett. **14**, 147–156 (2002)
25. Thirouard, B., Tian, T.: Oil transport in the piston ring pack (part I): identification and characterization of the main oil transport routes and mechanisms. *SAE Technical Paper 2003-01-1952* (2003).
26. Day, L., Dunaevsky, V., McCormick, H.: Critical factors affecting oil consumption and deposit formation in engines and compressors come to light from research in two disciplines. Tribol Lubrication Technol, STLE **2008**, 31–39 (2008)
27. Przesmitzki, S., Tian, T.: Oil transport inside the power cylinder during transient load changes. *SAE Technical Paper 2007-01-1054* (2007).
28. Kato, M., Fujita, K., Suzuki, H., Baba, Y., Ishima, T., Obokata, T.: Analysis of lubricant oil film behaviour on the piston surface according with piston shapes by means of LIF and PIV. *SAE Technical Paper 2009-01-0003* (2009).
29. Edwards, C.F.: In: Chiu, H.H., Chigier, N. (eds.) Mechanics and combustion of droplets and sprays. Begell House Inc (1995)
30. Lawes, M., Lee, Y., Marquez, N.: Comparison of Iso-octane burning rates between single-phase and two-phase combustion for small droplets. Combust. Flame **114**, 513–525 (2006)
31. Dyson, C.J., Priest, M., Lee, P.M.: Simulating the misting of lubricant in the piston assembly of an automotive gasoline engine: the effect of viscosity modifiers and other key lubricant components. Tribol. Lett. (2022). https://doi.org/10.1007/s11249-022-01589-0
32. Lee, P.M., Priest, M., Stark, M.S., Wilkinson, J.J., Lindsay-Smith, J.R., Taylor, R.I., Chung, S.: Extraction and tribological investigation of top piston ring zone oil from a gasoline engine. Proc. IMechE: J. J. Eng. Tribol. **220**, 171–180 (2006)
33. Yasutomi, S., Maeda, Y., Maeda, T.: Kinetic approach to engine oil: 1, analysis of lubricant transport and degradation in engine system. Ind. Eng. Chem. Prod. Res. Dev. **20**, 530–536 (1981)
34. Clark, N. N., Tatli, E., Barnett, R., Wayne, W. S., McKain, D. L.: Characterization and abatement of diesel crankcase emissions. *SAE Technical Paper 2006-01-3372* (2006).
35. Tatli, E., Clark, N. N.: Crankcase particulate emissions from diesel engines. *SAE Technical Paper 2008-01-1751* (2008).
36. Johnson, B.T., Hargrave, G.K., Reid, B.A., Page, V.J., Wagstaff, S.: Optical analysis and measurement of crankcase lubricant oil atomisation. *SAE Technical Paper 2012-01-0882* (2012).
37. Johnson, B. T., Hargrave, G. K., Reid, B., Page, V. J.: Crankcase sampling of PM from a fired and motored compression ignition engine. *SAE Technical Paper 2011-24-0209* (2011).
38. Behn, A., Feindt, M., Matz, G., Krause, S.: Fuel transport across the piston ring pack: measurement system development and experiments for online fuel transport and oil dilution measurements. *SAE Technical Paper 2015-01-2535* (2015).
39. Dollmeyer, T.A., Vittorio, D.A., Grana, T.A., Katzenmeyer, J.R., Charlton, S.J., Clerc, J., Morphet, R.G., Schwandt, B.W.: Meeting the US 2007 heavy-duty diesel emission standards—designing for the customer. *SAE Technical Paper 2007-01-4170* (2007).
40. Begg, S.M., De-Sercey, G., Miche, N.D.D., Heikal, M.R., Gilchrist, R., Noda, Y., Tsuruoka, Y., Mamiya, Y.: Experimental investigation of the phenomenon of oil breakup in an engine crankcase. Atomization Sprays **20**, 801–819 (2010)
41. Wang, Z., Yi, P., Qu, W., Feng, L., Gong, Z.: Numerical simulation of monodisperse lube oil multiple droplet evaporation and autoignition under nonconstant cylinder conditions of low-speed two-stroke gas engines. ACS Omega **2021**, 33568–22582 (2021)
42. Marano, R. S., Messick, R. L., Smolinold, J. M., Toth, L.: SAE Technical Paper 950245 (1995).
43. Lee, P.M.: Measured piston and liner temperatures in a gasoline: part 1, effects of lubricant viscosity and throttle position. STLE Annual Meeting 2010, Las Vegas, USA (2010).
44. McKinley, G.H.: Dimensionless groups for understanding free surface flows of complex fluids. *SOR Rheology Bulletin* (2005).
45. Jeng, S.-M., Deng, Z.: In: Kuo, K.K. (ed.) Recent advances in spray combustion: spray combustion measurements and model simulation, vol. II. AIAA (1996)
46. Tanner, F. X.: A cascade and atomization and drop breakup model for the simulation of high-pressure liquid jets. *SAE Technical Paper 2003-01-1044* (2003).
47. Taylor, R.I.: Energy efficiency, emission, tribological challenges and fluid requirements of electrified passenger cars. Lubricants **9**, 66 (2021)
48. Reitz, R., Diwakar, R.: Effect of droplet breakup on fuel sprays. *SAE Technical Paper 860469* (1986).
49. Arcoumanis, C., Khezzar, L., Whitelaw, D.S., Warren, B.C.H.: Breakup of newtonian and non-newtonian fluids in air jets. Exp. Fluids **17**, 405–414 (1994)